JOURNAL OF TISSUE ENGINEERING AND REGENERATIVE MEDICINE
J Tissue Eng Regen Med (2015)
Published online in Wiley Online Library (wileyonlinelibrary.com) **DOI:** 10.1002/term.2080

RESEARCH ARTICLE

A bioartificial environment for kidney epithelial cells based on a supramolecular polymer basement membrane mimic and an organotypical culture system

Björne B. Mollet[1,2], Iven L. J. Bogaerts[1,2], Geert C. van Almen[1,2] and Patricia Y. W. Dankers[1,2]*
[1]*Department of Biomedical Engineering, Laboratory of Chemical Biology, Eindhoven University of Technology, The Netherlands*
[2]*Institute for Complex Molecular Systems, Eindhoven University of Technology, The Netherlands*

Abstract

Renal applications in healthcare, such as renal replacement therapies and nephrotoxicity tests, could potentially benefit from bioartificial kidney membranes with fully differentiated and functional human tubular epithelial cells. A replacement of the natural environment of these cells is required to maintain and study cell functionality cell differentiation *in vitro*. Our approach was based on synthetic supramolecular biomaterials to mimic the natural basement membrane (BM) on which these cells grow and a bioreactor to provide the desired organotypical culture parameters. The BM mimics were constructed from ureidopyrimidinone (UPy)-functionalized polymer and bioactive peptides by electrospinning. The resultant membranes were shown to have a hierarchical fibrous BM-like structure consisting of self-assembled nanofibres within the electrospun microfibres. Human kidney-2 (HK-2) epithelial cells were cultured on the BM mimics under organotypical conditions in a custom-built bioreactor. The bioreactor facilitated *in situ* monitoring and functionality testing of the cultures. Cell viability and the integrity of the epithelial cell barrier were demonstrated inside the bioreactor by microscopy and transmembrane leakage of fluorescently labelled inulin, respectively. Furthermore, HK-2 cells maintained a polarized cell layer and showed modulation of both gene expression of membrane transporter proteins and metabolic activity of brush border enzymes when subjected to a continuous flow of culture medium inside the new bioreactor for 21 days. These results demonstrated that both the culture and study of renal epithelial cells was facilitated by the bioartificial *in vitro* environment that is formed by synthetic supramolecular BM mimics in our custom-built bioreactor.

Received 27 July 2014; Revised 18 May 2015; Accepted 23 June 2015

Keywords **kidney epithelial cell; bioreactor; *in vitro* test; flow culture; basement membrane mimic; supramolecular biomaterial**

1. Introduction

Kidney tubular epithelial cells play an essential role in maintaining homeostasis by exerting endocrine, metabolic and specific transport functions. These cells could potentially aid medical applications, such as establishment of *in vitro* nephrotoxicity tests (Tiong *et al.*, 2014; Pfaller and Gstraunthaler, 1998) and improvement of renal replacement therapies (Aebischer *et al.*, 1987; Fissell *et al.*, 2006; Humes, 2000; Saito *et al.*, 2011). Such applications would benefit most from viable renal tubule cells in a highly differentiated and functional epithelial phenotype, grown as a confluent layer on a membrane outside the human body. However, tubular epithelial cells are prone to losing their characteristic confluent monolayer morphology and specific functions when cultured *in vitro* (Fujita *et al.*, 2002; Ozgen *et al.*, 2004). It is expected that optimal cell function will be retained when these cells are cultured *in vitro* in a bioartificial environment that is

**Correspondence to: Patricia Y. W. Dankers, Den Dolech 2, 5612 AZ Eindhoven, The Netherlands. E-mail: P.Y.W.dankers@tue.nl*

ideally indistinguishable from the cells' natural environment, as perceived by the cell. Such an *in vitro* environment would comprise: (a) an appropriate membrane surface for the cells to grow on (Kirkpatrick, 2014); and (b) an organotypical culture environment (Figure 1).

The natural surface on which renal epithelial cells grow is formed by the basement membrane (BM). This specialized type of dense extracellular matrix (ECM) provides mechanical strength to epithelial tissues and maintains stable tissue borders. Main components of the BM are collagen IV and laminin, which form hierarchical fibrillar assemblies and complex networks with the aid of crosslinking proteins (Timpl, 1996). Due to the supramolecular nature of protein–protein interactions, the BM has an inherently dynamic character, which allows responsive interaction with cells (Timpl and Brown, 1996). Furthermore, the BM provides bioactive cues to the epithelial cells, such as ligands that are recognized by the integrin cell-surface receptors, which facilitate cell anchorage to the BM (Timpl, 1996).

The applicability of natural basement membranes in *in vitro* settings is very limited, since these structures are difficult to isolate and process as freestanding membranes. Therefore, in earlier endeavours to establish *in vitro* BM substitutes for renal cells mechanically stable synthetic polymer materials were used (Saito *et al.*, 2011; Humes *et al.*, 1999; Ni *et al.*, 2011; Schophuizen *et al.*, 2015). Since synthetic materials generally do not provide bioactive cues, lack dynamics and do not assemble into hierarchical fibrous structures, these materials were often combined with a bioactive coating of natural origin. However, the limitations of naturally derived components, such as restricted accessibility at large scales and variability of content, pose limitations for their use in future medical applications.

Therefore, in our study we have focused on a fully synthetic approach towards an *in vitro* BM substitute which is based on supramolecular building blocks. In supramolecular polymers the monomeric units polymerize via noncovalent, dynamic interactions (Aida *et al.*, 2012). This provides opportunities to form tunable and instructive biomaterials that are more natural-like. The monomeric units in our material system consist of commercial polymers or oligomers that are functionalized with self-complementary four-fold hydrogen bonding 2-ureido-4[1*H*]-pyrimidinone (UPy) moieties (Sijbesma *et al.*, 1997). Hence, supramolecular polymerization occurs via spontaneous UPy-dimerization, which is a strong but still dynamic interaction ($K_{dim} = 6 \times 10^7$/M in chloroform) (Söntjens *et al.*, 2000). Because the unifying UPy-moiety bioactivation of UPy-polymer materials is readily accessible via the introduction of UPy-functionalized peptides (Figure 2) (Kieltyka *et al.*, 2012; Dankers *et al.*, 2011), multiple UPy-polymers and UPy–peptides can be mixed to form materials with specific properties (Mollet *et al.*, 2014). This approach enables the formation and exploration of new synthetic materials that can substitute the BM in *in vitro* applications.

In the present study we focused on the morphological aspects of BM mimicry by using UPy-based biomaterials. This was an important aspect, since naturally occurring nanotopographic structures within extracellular matrices present the surrounding cells with cues that influence cell behaviour (Andersson *et al.*, 2003). For example, epithelial cell morphology and cytokine production were indicated to depend on the underlying nanotopography (Bettinger *et al.*, 2009). For various UPy-functionalized polymers, nanofibrillar structures have been identified on the surface of drop-cast films (Kautz *et al.*, 2006). These structures are the result of an hierarchical self-assembly process which encompasses UPy-dimerization, UPy-dimer stacking (van Beek *et al.*, 2007) and stack aggregation (Appel *et al.*, 2011). Since the self-assembly process is encoded in the molecular design of UPy–urea-functionalized building blocks, a BM-like hierarchically self-assembled nanostructure is likely to be within reach using the UPy-based biomaterial system. When combined with electrospinning to form microfibres, a hierarchical

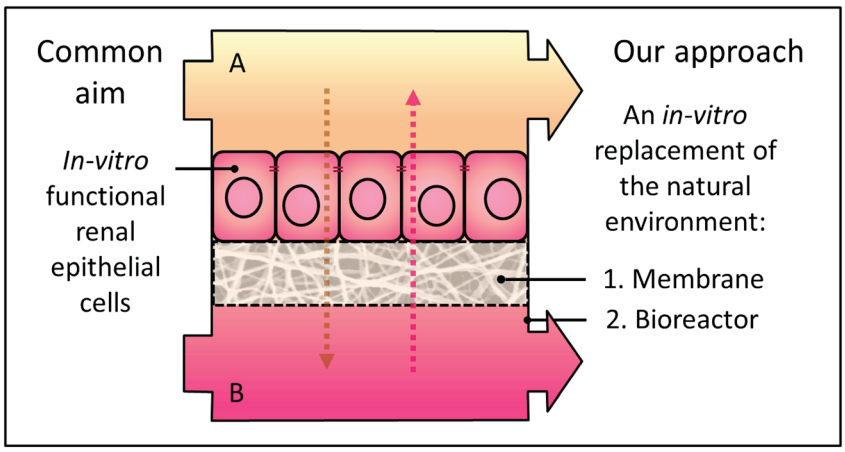

Figure 1. A schematic representation of our approach towards *in-vitro* functional renal epithelial cells: the development of a bioartificial environment for kidney epithelial cells, which is formed by a basement membrane mimicking synthetic culture substrate (1) and a bioreactor that provides an organotypical culture environment (2). In this bioreactor, the basement membrane mimic is placed between two compartments, which can each be provided by a separate flow of media. The membrane side at which the renal epithelial cells are situated, is referred to as the 'apical side' (A), the other side of the membrane is referred to as the 'basal side' (B).

DOI: 10.1002/term

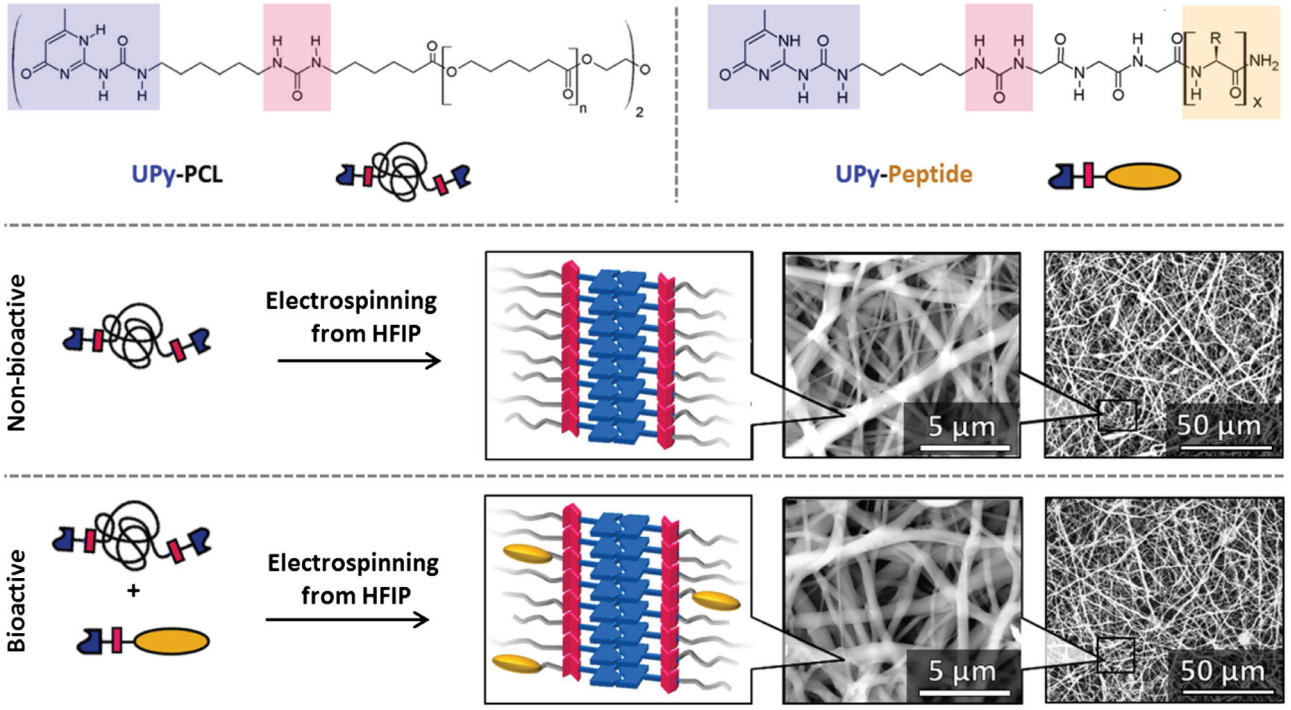

Figure 2. Chemical structures of supramolecular biomaterial building blocks UPy-PCL (top, left) and UPy-peptide (top, right), both with a urea linker, indicated in red. UPy-PCL was electrospun from HFIP without (middle) and with a mixture of four different UPy-peptides (bottom) to make non-bioactive and bioactive microfibrous membranes, respectively. Scanning electron micrographs show submicron fiber diameters (non-bioactive: 0.44 µm ± 0.22 µm, bioactive: 0.34 ± 0.22 µm), apparent pore sizes smaller than 5 µm and an overall homogeneous morphology of the membranes. The electrospun microfibers are proposed to contain self-assembled UPy-dimer stacks.

fibrous nano–microscale structure is expected to result. However, to the best of our knowledge this has never been demonstrated. The effect of both electrospinning and the addition of monofunctional bioactive UPy–peptides on the formation of self-assembled nanostructures was investigated in the present study.

Besides an appropriate synthetic basement membrane, the ideal *in vitro* culture environment for renal epithelial cells should provide organotypical culture conditions. Bioreactors have been developed and applied to create organotypical culture conditions *in vitro* for a diversity of organs, such as the bronchiole (Miller *et al.,* 2010) or intestine (Kim *et al.,* 2007). Characteristic for kidney tissue is the (pre)urine and blood flow, between which the renal epithelial cells are located to exert their functions. *In vitro*, this translates to the requirement of a continuous flow of separate media at each side of the BM, mimicking the membrane on which the renal epithelial cells are cultured. Devices dedicated to mimicking a small part of the kidney tubular structure have been reported (Sciancalepore *et al.*, 2014; Jang and Suh, 2010; Baudoin *et al.*, 2007). Although these so-called 'organs-on-chip' facilitate the culture of renal epithelial cells under flow conditions, they do not allow culture on different material surfaces or are limited in the type of surface that can be used. A bioreactor design that allows the easy application of different membrane materials, but which is limited to the application of culture medium at one side of the membrane, was described by Sun *et al.* (2012). Another interesting microfluidic bioreactor, presented by Ferrell *et al.* (2010), established renal epithelial cell culture on thin membranes under the application of flow via microfluidic channels at the apical side. Only a limited number of bioreactors that provide a culture environment suitable for renal epithelial cells are commercially available. The ones that allow a free choice of support material and application of flow at each membrane side are, to our knowledge, limited to the culture systems of Minucells and Minutissue GmbH (Minuth *et al.*, 2009; Minuth and Denk, 2015). However, none of these systems meet the exact requirements that are desired for the cell studies on our UPy-based BM mimics. Those requirements include: (a) compatibility with different types of BM mimic; (b) the possibility of applying a separate flow of medium to each side of the BM mimic; (c) *in situ* visualization by microscopy to allow monitoring of the culture in time; (d) sufficient volume of the compartment at each side of the membrane to allow the use of the bioreactor for static cultures and, in addition, to provide the opportunity to perform different assays on the incubated media: and, furthermore, basic requirements, such as: (e) the possibility of thoroughly cleaning and sterilizing the bioreactor; (f) the need for the bioreactor to be leak-free, both externally and internally (i.e. no connection between the media at each side of the membrane other than through the membrane); and lastly (g) that the design should be optimized to prevent adverse effects of air bubbles that tend to form and accumulate in such flow-culture systems. According to these requirements, we developed a custom-built bioreactor system that allows both the culture and assessment of living bioartificial renal tubular membranes *in vitro*. In this paper,

DOI: 10.1002/term

we describe the design and initial validation tests of this new bioreactor system in conjunction with the use of our synthetic UPy-based BM mimics.

2. Materials and methods

2.1. Preparation and characterization of non-bioactive and bioactive UPy–PCL membranes

2.1.1. Membrane electrospinning

A home-built electrospinning set-up equipped with a syringe pump (KD Scientific) was used. The supramolecular UPy–PCL polymer and UPy–peptides were synthesized, as described previously (Dankers *et al.*, 2011). For non-bioactive membranes, 15 w/w% UPy–PCL was dissolved in 85 w/w% 1,1,1,3,3,3-hexafluoro-2-propanol (HFIP; 147545000, Acros). For bioactive UPy–PCL meshes, a mix of four UPy–urea (UPy-U) functionalized peptides was added. The four peptides, GRGDS (Pierschbacher and Ruoslahti, 1984), PHSRN (Aota *et al.*, 1994), DGEA (Staatz *et al.*, 1991) and YIGRS (Iwamoto *et al.*, 1987), are based on cell-binding epitopes of ECM proteins. The bioactive electrospin solution was prepared by dissolution of 0.5 mol% of each of the UPy-U peptides (2 mol% UPy–peptides in total) with respect to polymer in the appropriate amount of HFIP (85 w/w%), prior to the addition of 15 w/w% UPy–PCL. The polymer solution was transferred to a syringe and fed to a blunt-ended 23 G needle via PTFE 1 mm i.d. tubing at a rate of 0.02 ml/min and electrospun by the application of 18.5 kV between a tip-to-target distance of 12 cm. The electrospun fibres were collected randomly on a glass plate that covered the grounded collector. The resultant membranes were gently removed from the glass and placed *in vacuo* at 40 °C overnight to remove any residual solvent. The microscale morphology of the fibrous membranes was analysed using scanning electron microscopy (SEM) on a FEI Quanta 600 ESEM with Xt Microscope Control software. Samples were directly imaged (without a conducting coating) in low-vacuum mode (~1 mbar) with an applied voltage of 15 kV. Both secondary electrons and backscattering electrons were detected and the separately recorded images were merged to false-coloured images.

2.1.2. Atomic force microscopy (AFM) on UPy–PCL drop-cast and electrospun surface

Atomic force microscopy (AFM) measurements were performed on a Digital Instrument Multimode Nanoscope IV, using PPP-NCHR-50 silicon tips (Nanosensors) in the soft tapping mode (280–290 kHz) at room temperature. The nanoscale surface morphology of both electrospun microfibres and a film of UPy–PCL was visualized. The film was made by casting a few drops of a solution of 1 mg/ml UPy–PCL in chloroform on glass coverslips, followed by annealing *in vacuo* at 40 °C overnight. The electrospun UPy–PCL fibres were prepared as described above. Both fibres in a self-supporting mesh and separate fibres collected on a glass cover slip were imaged, as described previously (Appel, 2011).

2.1.3. Wide-angle X-ray scattering (WAXS) on UPy–PCL

WAXS measurements were performed at the European Synchrotron Radiation Facility (ESRF) in Grenoble, France, at the DUBBLE beamline (BM26b), using a 2657 × 3955 pixels VHR detector) (Photonic Science). Measurable dimensions were 1–15 Å. Samples were prepared by filling aluminium sample pans with polymer material – either the white solid, as obtained from precipitation in heptane in the last step of UPy–PCL synthesis, or this polymer processed into a microfibrous mesh by electrospinning from HFIP, with or without 2 mol% UPy–peptides. For comparison, non-UPy functionalized PCL (2000 g/M), as received from the manufacturer, was added to the sample group. Measurements were performed at room temperature.

2.2. Bioreactor design and fabrication

The bioreactor was designed to hold a single biomaterial membrane, free of choice. The bioreactor was assembled from separate custom-made components (Figure 3). Two central parts were: (a) constructed from polyether ether ketone (PEEK), which was chosen for its excellent thermal and chemical resistance to allow repeated sterilization by steam or chemicals; together the central parts fitted (b) a silicone rubber membrane carrier, which was inspired by the Minusheet carrier (Minucells and Minutissue, Bad Abbach, Germany). This membrane carrier fitted a single, round, 11–13 mm diameter membrane and left 8.9 mm dismeter of the membrane available for cell seeding. In addition it functioned as a silicone rubber O-ring between the two central parts to facilitate leak-free assembly. The membrane placed inside the bioreactor divides the system into two separate chambers. These chambers, each provided with an inlet and outlet (1 mm i.d., 3 mm o.d.), allowed separate flow of medium on both sides of the membrane. Each chamber was closed with a 0.7 mm thick, 27 mm diameter glass window (4), which provides visual access to the membrane and the chamber. Rings cut from 1.0 mm-thick silicone rubber sheet (3), were placed between the central parts and the glass windows to provide leak-free assembly. PEEK lids (5) were applied to hold the glass windows in place. Twelve stainless steel screws were used for assembly of the bioreactor; four to fix the two central parts and four to fasten each lid. A closed-flow system was formed by connecting the bioreactor inlets and outlets via silicone rubber tubing (2 mm i.d.: Rubber BV, The Netherlands), polypropylene luer and barbed tubing connectors (Qosina, USA) and a

DOI: 10.1002/term

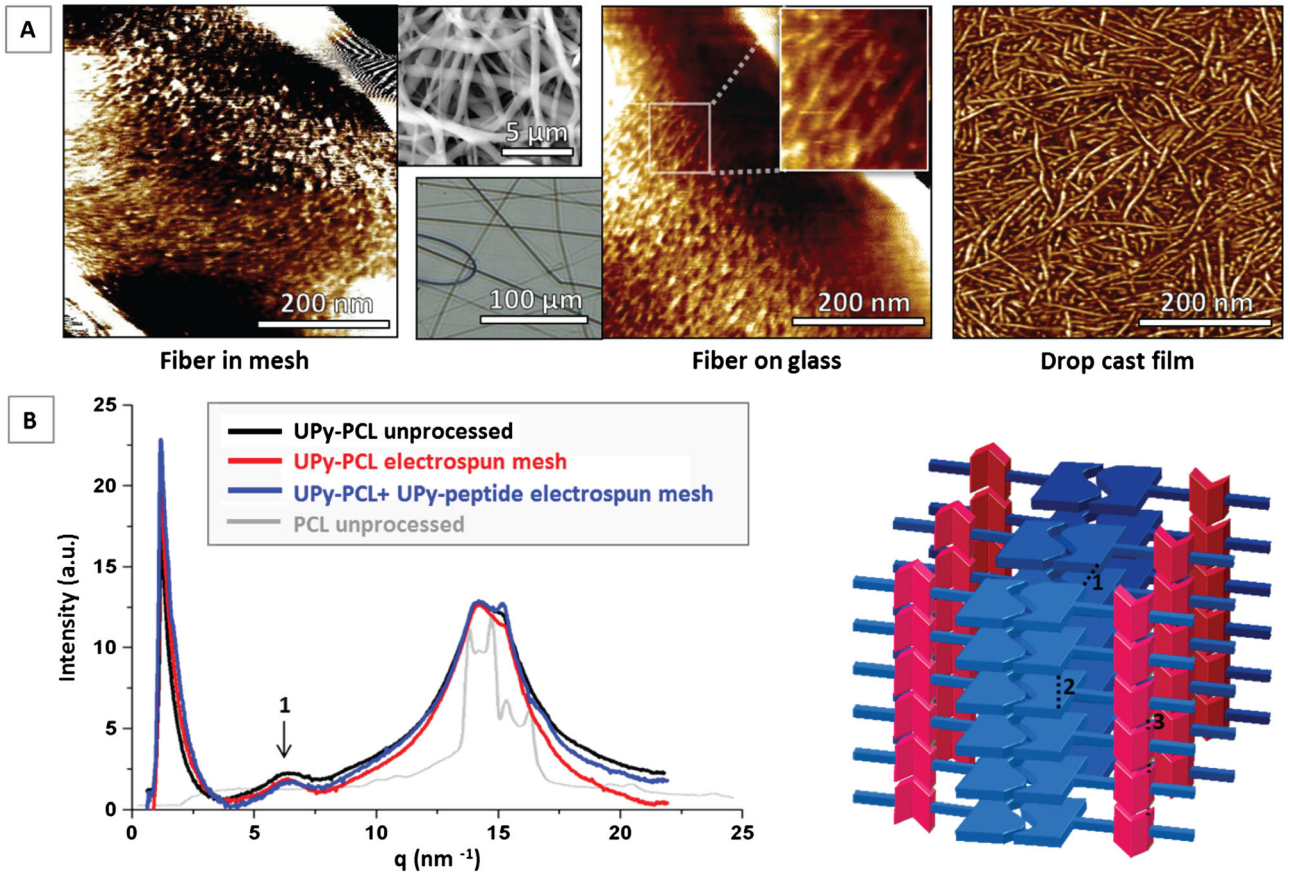

Figure 3. Structural organization at the nanoscale within UPy-PCL microfibers. (A) AFM phase images of UPy-PCL surfaces prepared from HFIP; an electrospun microfiber in either a mesh (left, SEM micrograph attached) and on a flat glass surface (middle, brightfield micrograph attached) and a drop-cast film (right). Phase separated nanofibers, attributed to the hard UPy-urea stacks are best observed in the drop-cast film. Relatively large height differences in the electrospun mesh hamper accurate imaging with AFM. However, nanofibrous structures are present and can be observed on the surface of electrospun UPy-PCL microfibers, as demonstrated for single fibers collected on the flat glass substrate. (B) WAXS shows the diffraction pattern due to ordered structures in UPy-U stacks, schematically depicted on the right. Three UPy-PCL samples were compared with non-functionalized, unprocessed PCL (as received from the supplier). The intensity of the diffraction pattern of PCL was scaled to allow better comparison with the diffraction patterns of UPy-PCL samples and does not correspond to the indicated intensity in the graph (max. signal PCL was ~100).

polycarbonate medium reservoir. The medium reservoir was equipped with three openings that fitted male Luer slip connectors, one in the lid to fit a standard 0.2 µm pore syringe filter for sterile ventilation, and two to connect medium inflow and outflow tubing. Medium flow was driven by a tubing pump, resistant against the humid environment (IP65 rated, Ismatec MCP process, equipped with MS/CA 4–12 pumphead and extension blocks; Inacom) inside a cell incubator. Up to 12 separate bioreactor flow systems could be attached to this pump simultaneously. All unassembled bioreactor and flow circulation parts were sterilized by steam autoclaving for 20 min at 121 °C prior to use in any cell experiment.

2.3. Human kidney-2 cell culture and seeding on membranes

Human kidney-2 (HK-2) cells were routinely cultured in culture flasks in a complete medium consisting of Dulbecco's modified Eagle's medium (DMEM; Gibco, Invitrogen) supplemented with 10 v% heat-inactivated fetal bovine serum (FBS; 26140-079, Gibco, Invitrogen) and 1 v % penicillin–streptomycin solution (Gibco). The medium was refreshed every 2–3 days. Circular membranes with a diameter of 12 mm were punched from the electrospun meshes and sterilized by exposure to UV light (1 h/side). Each membrane was clamped in a membrane carrier and transferred to a well plate; for static control cultures, Minusheet (1300, Minucells and Minutissue) were used in 24-well plates; for studies inside the bioreactor, silicone rubber carriers were used in a 25 square well plate (Sterilin, Beldico, Duiven, The Netherlands). Each membrane was wetted in an ample volume of complete medium, then the medium was removed until the fluid level reached the upper surface of the carrier, followed by removal of residual medium on top of the membrane. 3×10^5 HK-2 cells in 75 µl/membrane were seeded within the opening of the membrane carrier ring (8.9 mm i.d. for both Minusheet and silicone rubber membrane carriers). The cells were left to adhere for 2 h at 37 °C and 5% CO_2 in a humidified atmosphere. Then, 700 µl complete medium was added to each well and the cells were precultured under static culture

DOI: 10.1002/term

conditions at 37 °C and 5% CO_2 in a humidified atmosphere. The medium was refreshed every other day. The length of the preculture time is indicated in the experiment.

2.4. Validation of the bioreactor in cell culture and assessment

2.4.1. Monitoring cells inside the bioreactor: in situ microscopy

In situ cell viability inside the bioreactor was visualized via a live/dead assay (L3224, Invitrogen). HK-2 cells, statically cultured on a non-bioactive UPy–PCL membrane, were incubated for 15 min at 37 °C in complete medium supplemented with 10 μM calcein AM and 10 μM ethidium homodimer and washed with phosphate-buffered saline (PBS). The membrane was placed inside a bioreactor, which was then filled with complete culture medium and incubated further under static conditions at 37 °C and 5% CO_2. Imaging of the cells inside the bioreactor was performed using an inverted fluorescence microscope, using a Zeiss Axio observer D1, AxioCam Mrm camera and Zeiss Axiovision software (Carl Zeiss), at different times after staining. Three objectives with working distances (WDs) based on standard 0.13 mm thick glass cover-slips and air as barrier between the objective and specimen) > 3.9 mm were tested for imaging (A-Plan ×10, NA 0.25, WD 4.4; LD A-Plan ×20, NA 0.30, WD 4.3; LD plan neofluar ×20 korr, NA 0.40, WD 7.9, all from Zeiss).

2.4.2. Transmembrane inulin diffusion: cell monolayer integrity

Porous electrospun non-bioactive UPy–PCL membranes were first sterilized and thoroughly pre-wetted by submersion in PBS for at least 3 days. The membranes ($n = 13$) were first placed inside the bioreactors and tested without cells, prior to testing the same membranes with cells. The chambers were filled with separate media. The chamber on the side of the membrane to which cells will be seeded, referred to as the 'apical side', was first filled with complete culture medium. The chamber on the side of the membrane to which no cells will be seeded, referred to as the 'basal side', was filled with complete culture medium supplemented with 5 mM inulin-FITC (FI 100 mg, MW 4.5 kDa; TdB Consultancy AB, Uppsala, Sweden). The inlets and outlets were closed and the bioreactors were placed in a humidified atmosphere for 4 h at 37 °C and 5% CO_2. Then the medium from each chamber was collected separately, vortexed and three 200 μl samples were transferred to a black flat-bottomed 96-well plate (Thermo Scientific) and fluorescence was measured ($\lambda_{ex} = 495$, $\lambda_{em} = 515$) using a fluorescence microplate reader (Safire 2, Tecan). The membranes were washed with PBS and the procedure was repeated at three later times points on the same membranes; first with an incubation time of 24 h, then with cells seeded on the membranes and subsequent incubation times of 4 h and 24 h. For the experiment with cells, 3×10^5 HK-2 cells/memebrane were seeded on the apical side. The cells were allowed to form a confluent monolayer during a preculture period under static conditions for 2 days before the diffusion test was repeated. The 5 mM FITC–inulin in the medium that was applied to the basal side was chosen such that it was within the linear regime of concentration-dependent fluorescence intensity. The percentage of diffused FITC–inulin was calculated from the measured fluorescence signals [fluorescence apical × 100%/(fluorescence basal + fluorescence apical)] for each membrane at each time point, 4 and 24 h, and for each condition, without and with cells. From those percentages, the averages and standard errors were determined (result expressed in absolute values is available in the supporting information, Figure S1). Diffusion in the presence and absence of cells was compared for both incubation times separately via an unpaired two-sample *t*-test; error bars represent standard error of the mean (SE); $p < 0.05$ was considered statistically significant.

2.4.3. Cell culture under flow conditions inside the bioreactor

Bioactive UPy–PCL membranes with HK-2 cells were precultured under static conditions for 4 days before subjection to a continuous flow inside separate bioreactors for 21 days. Each bioreactor was attached to a container with 9 ml complete medium. Medium was circulated through the closed system via peristaltic tubing pump (Ismatec) and flowed over the membrane through both the apical and basal chambers at a 6 ml/h flow rate. The bioreactors were arranged vertically, with the outflow of both chambers pointing upward to allow easy removal of any air bubbles that might enter the chambers. The set-up was placed as a whole in a cell incubator (Thermo Scientific), which maintained 37 °C, 5% CO_2 and a humidified atmosphere. As a control, other cell-seeded membranes were further cultured in 24-well plates under static culture conditions with complete medium refreshment every 2–3 days.

2.4.3.1. Cell viability: mitochondrial activity assay. To assess cell viability, a mitochondrial activity assay was used, based on the mitochondrial conversion of non-fluorescent resazurin to fluorescent resorufin. Resazurin salt (Sigma-Aldrich) was dissolved in complete medium in a 4.4×10^{-5} M concentration. The membranes with HK-2 cells were incubated at 37 °C and 5% CO_2 in a humidified atmosphere with 800 μl resazurin solution for 2 h. For each membrane, three volumes 200 μl resazurin solution were then transferred to a black 96-well plate (Thermo Scientific) and fluorescence was measured ($\lambda_{ex} = 550$, $\lambda_{em} = 584$) using a Fluoroscan plate reader (Thermo Fisher Scientific). All data were expressed as mean ± SE. The average total mitochondrial activity for static cultures in time ($n = 5$ during the preculture period, days 1–4, $n = 3$ at day 25) was evaluated using ANOVA. Comparison of the flow samples

DOI: 10.1002/term

($n = 2$) with static samples at days 1 and 25 was performed via separate two-sample *t*-tests; $p < 0.05$ was considered statistically significant.

2.4.3.2. Cell morphology: fluorescent immunostaining of tight junctions. The formation of tight junctions between cells was evaluated via immunofluorescent zona occludens 1 (ZO-1) protein staining, combined with a nuclear counterstain. After the culture period, the cells were washed twice with PBS, fixed with 2% formaldehyde (Fluka)/PBS for 10 min and again washed twice with PBS. The fixed cells were stored in PBS at 4 °C until further use. To block non-specific binding sites, the samples were incubated with 5% w/v BSA in PBS for 30 min at room temperature. The cells were incubated with mouse anti-ZO-1 antibody (1:200; 610966, DB Biosciences Pharmingen) for 1 h and sequentially with rabbit anti-mouse fluorescein isothiocyanate (RAM-FITC; 1:100; Dako) and 4,6-diamidino-2-phenylindole (DAPI; 1:1000; Sigma-Aldrich) in PBS with 5 w/v% BSA for 30 min at room temperature. The stained membranes were embedded in CitiFluor (Agar Scientific) between a glass microscopy slide and a coverslip and visualized with fluorescence microscopy, using a Zeiss Axio observer D1, AxioCam Mrm camera and Zeiss Axiovision software (Carl Zeiss).

2.4.3.3. Gene expression: quantitative reverse transcription–polymerase chain reaction (RT–PCR). The gene expression levels of specific membrane transporters were determined in HK-2 cells cultured on bioactive UPy–PCL membranes. Flow cultures (4 days static preculture + 21 days flow culture; $n = 5$) were compared to static cultures ($n = 7$) at day 25 after cell seeding on bioactive UPy–PCL membranes. Total RNA was isolated using High Pure RNA Isolation Kit (Roche), according to the manufacturer's instructions, and cDNA was synthesized. Transcript levels for *SGLT2*, Na^+/H^+ ATPase, *Pept 1*, *Pept 2*, *OCT 1* and *OAT 3* (primers were designed using free software from PubMed/NCBI; sequences are listed in the supporting information, Table S1) were detected using the MyIQ Single Color Real-Time PCR Detection System (Bio-Rad, Hercules, CA, USA), using SYBR green. All expression levels after 40 amplification cycles were presented relative to glyceraldehyde 3-phosphate dehydrogenase (*GAPDH*) and normalized to static culture conditions. All data were expressed as mean ± SE; $p < 0.05$ was considered statistically significant.

2.4.3.4. Metabolic activity: brush border enzyme activity. The metabolic activity of three brush border enzymes was determined for HK-2 cells cultured on bioactive UPy–PCL membranes. Flow cultures (4 days static preculture + 21 days flow culture; $n = 3$) were compared to static cultures ($n = 4$) at day 25 after cell seeding on bioactive UPy–PCL membranes. Cell lysates of the cultures were acquired by freeze–thawing each sample in 400 µl 5 mM Tris–HCl buffer with 0.9% NaCl and pH 7.4. The activity of brush border enzymes was assayed via the formation of 4-nitroaniline products, which adsorb at 405 nm. Kinetic colorimetric measurements were performed for 2–3 h at 37 °C, using a platereader (Safire 2, Tecan) on triplicate samples, each containing 10 µl cell lysate suspended in 200 µl substrate solution. γ-Glutamyl transferase activity was determined by the transfer of γ-glutamyl from L-glutamic acid 5-(3-carboxy-4-nitroanilide) to glycyl–glycine (Sigma-Aldrich). The concentration of the resultant 3-carboxy-4-nitroaniline in time was calculated from absorption measurements (Lambert-Beer equation: $A = \varepsilon \cdot c \cdot l$ with $\varepsilon = 9500$ mM/cm). Alkaline phosphatase activity was determined by following the dephosphorylation of 4-nitrophenyl phosphate (Sigma-Aldrich). Alanine aminopeptidase activity was determined by the conversion of L-alanine-4-nitroanilide (Sigma-Aldrich). The concentration of the resultant 4-nitroaniline in both these assays was determined according to the absorbance of a concentration series of 4-nitroaniline. The brush border enzyme activities were standardized with respect to the total amount of protein present in the cell lysate volume, which was determined using the Bradford assay, using bovine serum albumin (BSA) as reference (Bradford, 1976). The mean ± SE of enzymatic activity/sample group was expressed in nM/min/mg protein. In two-tailed *t*-test, $p < 0.05$ was considered statistically significant.

3. Results

3.1. Microfibrous electrospun UPy–PCL membranes

3.1.1. Electrospun non-bioactive and bioactive UPy–PCL membranes

UPy–PCL, both with and without bioactive peptides, was successfully electrospun from HFIP and yielded opaque white self-supporting porous membranes. SEM images showed the microfibrous morphology of randomly orientated fibres with typical sub-µm diameters, 0.44 ± 0.22 µm for the non-bioactive UPy–PCL membrane and 0.34 ± 0.22 µm for the bioactive UPy–PCL membrane (Figure 2). These fibre diameters gave rise to densely packed, porous meshes with apparent pore sizes < 5 µm. This was considered appropriate to allow renal epithelial to grow on top of, rather than inside, these microfibrous membranes.

3.1.2. Hierarchical fibrous structures in electrospun UPy–PCL

AFM was performed to confirm the presence of a nanoscale sub-structure within the electrospun UPy–PCL microfibres. This technique has been routinely applied to the surface of drop-cast films of UPy-polymers and

DOI: 10.1002/term

allows the identification of nanofibrillar structures, which have been attributed to hard, phase-separated, self-assembled UPy-stacks (Kautz *et al.*, 2006; van Beek *et al.*, 2007). The identification of nanostructures by AFM on microfibres of electrospun membranes proved to be challenging, due to the irregular surface of these samples at the microscale. The irregularity was diminished by the collection of single electrospun fibres on a flat glass surface. The curvature of the single fibre still hampered the detection accuracy of the AFM tip; nonetheless, distinct nanofibrils were observed (Figure 3a).

The presence of ordered UPy–urea structures within electrospun microfibres was confirmed by WAXS measurements (Figure 3b). Similar diffraction patterns were observed for UPy–PCL, before and after processing with electrospinning and in the presence of UPy–peptides. There were several small peaks superimposed on the alkyl halo of the diffraction pattern. These can be attributed to both crystalline PCL domains and UPy-U stacks. However, one specific peak was observed in the diffraction signal of all UPy–PCL samples, which was absent in the diffraction signal of non-functionalized PCL. The peak, which corresponded to a correlation distance of ~ 1 nm, has previously been observed for multiple UPy–urea- and UPy-urethane-functionalized polymers and has been attributed to the repeating distance between aligned UPy-dimer stacks (Appel *et al.*, 2011; Wietor *et al.*, 2011).

3.2. Bioreactor design and validation

To create an organotypical flow culture environment for a bioartificial renal membrane, a bioreactor was designed and successfully manufactured. Photographs and a schematic cross-section of the bioreactor are shown in Figure 4. Primary design criteria were the possibilities of applying any flat support material and of culture under continuous-flow conditions. Furthermore, visual and microscopic accessibility to the membrane and sufficient volume of the culture compartments was desired. The materials used to construct the design were chosen based on durability and compatibility with standard sterilization procedures, to

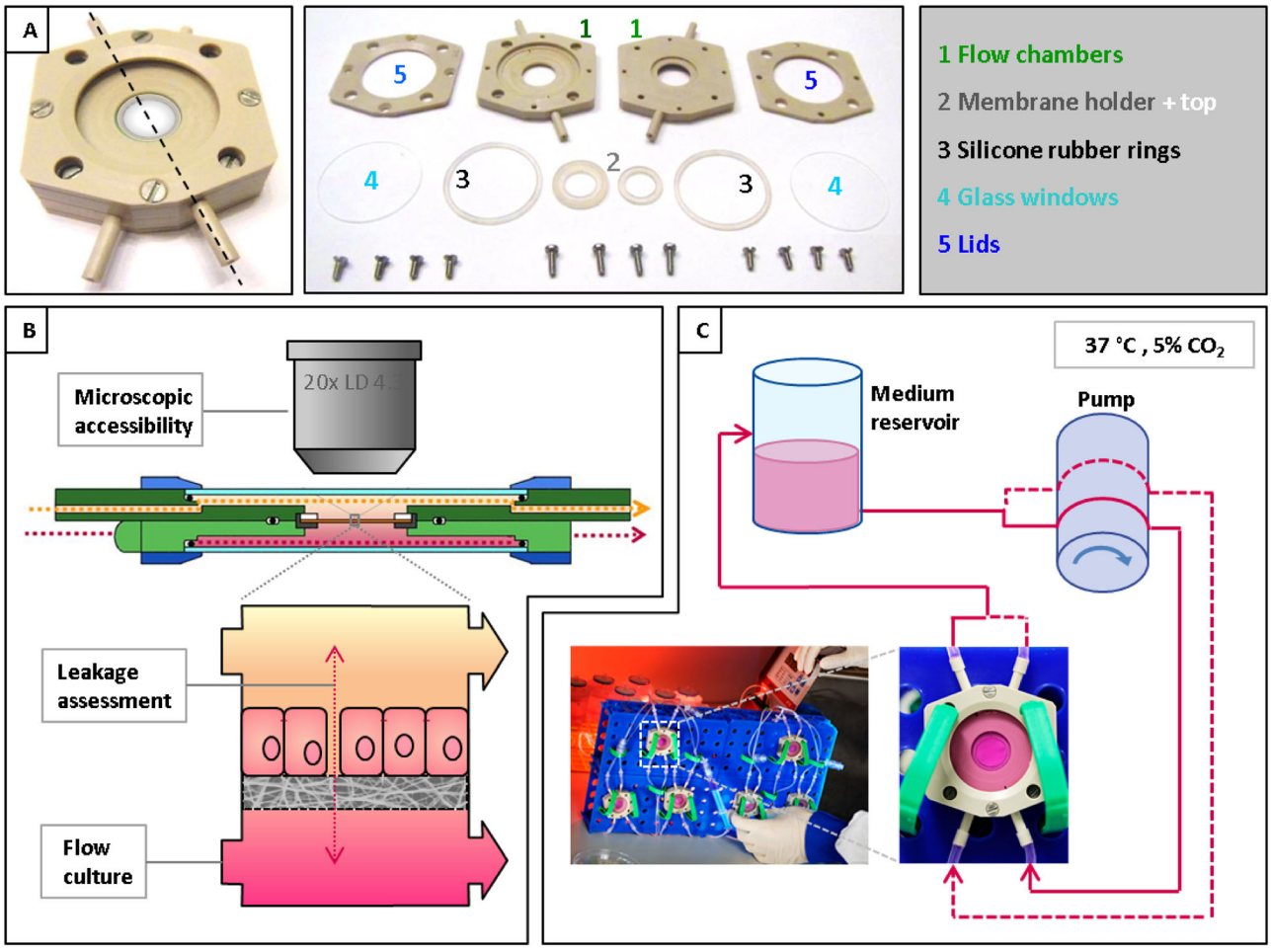

Figure 4. The custom-made bioreactor. (A) Photographs of the bioreactor in assembled and disassembled state. (B) A schematic, cross-section (indicated in A by the dotted line) of the bioreactor. The different parts are color coded, in correspondence with the legend. Different applications that were tested and described in the present work, are indicated. (C) A schematic representation of a total continuous flow culture setup, depicted here for one bioreactor that is provided with the same media in both the apical and basal flow-chamber. The bioreactor is placed vertically, connected to a reservoir with culture medium via silicone rubber tubing. A tubing pump can generate flow for multiple bioreactors at the same time. The complete assembly of multiple bioreactors, media reservoirs and the pump, as shown in the photograph, is placed inside an incubator at 37 °C and 5% CO_2.

DOI: 10.1002/term

allow re-usability of the bioreactor. The main parts of the bioreactor were constructed from PEEK, supplemented with glass windows, silicone rubber sealing rings and stainless-steel screws. In the disassembled state, the bioreactor could be thoroughly cleaned and sterilized repeatedly by autoclaving. Leak-tight assembly was verified in combination with a variety of support materials fixed inside the bioreactor, ranging in both thickness and stiffness. The possibility of modular assembly allowed the use of the bioreactor during different stages of a cell experiment. For example, with the upper lid still open, cells could be seeded exclusively on top of the fixed support material. After closing this lid, the bioreactor could be connected via the inlet and outlet of both chambers to a medium reservoir and pump using silicone rubber tubing. This allowed the culture of a bioartificial renal membrane under constant flow of media. The wide area inside the chambers at both sides of the membrane functioned as a buffer for any air bubbles that might result from the gas-permeable silicone tubing that was used to complete the media circulation. When an air bubble entered the flow chamber via the lower inlet, it freely moved upward to exit via the upper outlet (when the bioreactor was placed in a vertical position), without interfering with the membrane. The bioreactor was subjected to a series of experiments, in which HK-2 (Ryan *et al.*, 1994) cells were applied to the UPy–PCL-based membranes as a model for bioartificial renal tubule membranes.

3.2.1. *In situ* monitoring of cultures inside the bioreactor using microscopy

The bioreactor was designed with wide cross-section windows that allow visual access to the membrane and the surrounding chamber. Chamber height (distance between the membrane and the glass window) was minimized to further facilitate accessibility to the membrane by microscopy. The resulting distance that had to be bridged by the microscope objective was formed by a 3.2 mm-thick aqueous medium layer and a 0.7 mm-thick glass window. The possibility of *in situ* monitoring of cultures inside the bioreactor by microscopy was validated. A test culture with live/dead-stained HK-2 cells on opaque non-bioactive UPy–PCL membranes was placed inside the bioreactor. Fluorescence microscopy imaging proved to be successful, using low numerical aperture objectives (Figure 5). Successful visualization with maximum magnification and minimal working distance (WD) was achieved with a ×20 magnifying objective, with WD = 4.3 mm. The cells on the membrane inside the bioreactor remained well visible by fluorescence microscopy up to at least 2 days after the non-invasive live/dead staining (see supporting information, Figure S2).

3.2.2. Membrane leakage: diffusion test inside the bioreactor

The bioreactor was designed with a separate chamber at each side of the membrane culture. Hence, a membrane placed inside the bioreactor divides the system into two separate compartments that are connected through the porous membrane. This mimics the organotypical compartmentalization in the kidney. Via the application of medium with a different composition in each compartment, a compositional gradient can be applied. Thereby, diffusion or active transport of a particular substrate by the renal epithelial cells over the porous membrane can be studied. To demonstrate this possibility in the bioreactor, the difference in diffusion of fluorescein isothiocyanate-labelled inulin (FITC–inulin) over bare UPy–PCL membranes was compared to membranes seeded with HK-2 cells. Inulin has long been used as the standard to determine the kidney glomerular filtration rate (GFR). This compound is not bound to plasma proteins, is freely filtered in glomeruli and is neither reabsorbed nor secreted in the kidney's tubular track (Smith, 1951). Leakage of this compound through an epithelial cell monolayer was found to be a measure of the integrity of the tight-junction barrier (Madara and Dharmsathaphorn, 1985) and thus offers an opportunity to assess the formation of tight epithelial barriers *in vitro*.

The diffusion of FITC-inulin over pre-wet electrospun non-bioactive UPy–PCL membranes was measured in the absence of HK-2 cells and when covered with a presumably tight monolayer of HK-2 cells. After both 4 and 24 h of incubation at 37 °C, a significant decrease in FITC-inulin diffusion was observed over the electrospun UPy–PCL membranes when covered with epithelial cells (Figure 6). This indicated the formation of a near-tight cell layer at the apical side of the membrane, resembling the epithelial lining of kidney tubules.

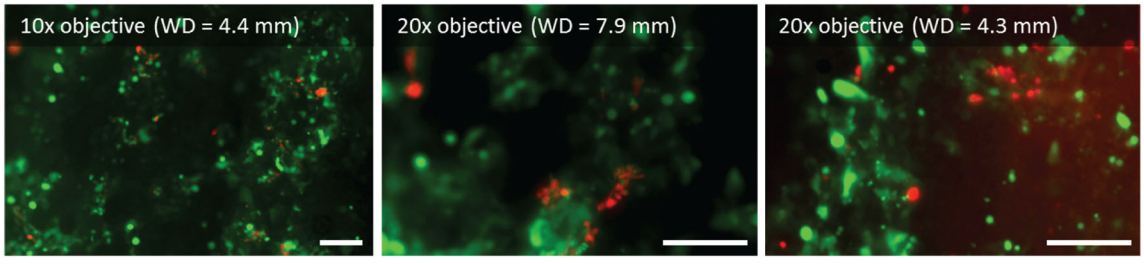

Figure 5. ***In situ*** **microscopy imaging. Fluorescence micrographs of live (green) / dead (red) stained HK-2 cells on an electrospun UPy-PCL membrane inside the bioreactor. The images were recorded with low aperture objectives with different magnification and working distance (WD). Scale bars represent 100 μm.**

DOI: 10.1002/term

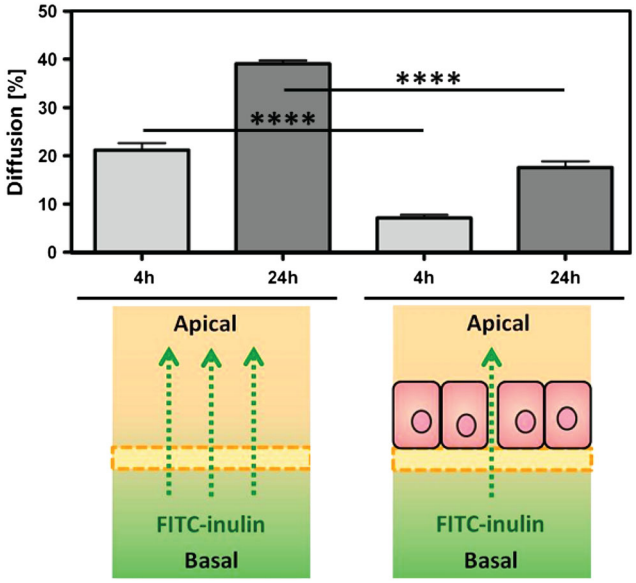

Figure 6. Epithelial cell layer integrity. Transmembranal FITC-inulin diffusion is determined as a measure for leakage (50% = maximum). Results are given for both 4 and 24 hours diffusion time at 37 °C through UPy-PCL membranes without and with HK-2 cells. The indicated significant differences between these sample groups correspond with $p < 0.0001$.

3.2.3. Effect of 3 weeks of flow culture on bioartificial renal tubule membranes

A continuous flow of sterile media was successfully established using the bioreactor culture set-up. This was utilized to culture bioartificial kidney tubule membranes under flow conditions. The effect of this culture method was compared to continued static culture. The test membranes consisted of HK-2 cells on bioactive UPy–PCL membranes. The HK-2 cells were seeded in a sufficiently high cell density to allow the instant formation of a confluent cell layer. The test membranes were precultured for 4 days under static conditions to allow the maturation of cells into a tight, polarized monolayer. This morphology was confirmed by fluorescent staining and microscopy visualization of zona occludens 1 (ZO-1) proteins in similar cultures (see supporting information, Figure S3). After static preculture, the membranes were subjected to a constant flow of culture media inside the bioreactors for 21 days. During this culture period, the bioreactors were regularly checked for adequate functionality at several basic criteria, such as leakage, air bubble accumulation and sterility. Absence of infection indicated that the separate parts had been successfully sterilized and remained sterile during assembly of the culture system. Absence of medium outside the system indicated proper leak-tight assembly. Air bubble formation in the system was expected and observed, but there were no signs of adverse effects (e.g. disruption of the membrane, discontinued flow) as a result of this. Cell viability, morphology and phenotype of the HK-2 cells were assessed after 3 weeks of flow culture inside the bioreactor and compared to static cultures of similar age.

3.2.3.1. Cell viability. Cell viability was indicated by both mitochondrial activity assay at set time points during the experiment (Figure 7) and live/dead staining after the total culture period of 25 days (see supporting information, Figure S5). The non-invasive mitochondrial activity assay is based on the uptake and mitochondrial conversion of non-fluorescent resazurin to fluorescent resorufin by viable cells. Equal fluorescence signals 1 day after cell seeding indicated equal seeding density throughout the separate bioartificial renal tubule test membranes (Figure 7). After the static preculture period of 4 days, the assay was repeated prior to subjection of parts of the cultures to media flow. Elevated total mitochondrial activity, indicative of elevated cell numbers, was observed throughout the cultures compared to day 1. After 21 days of flow culture, the average total mitochondrial activity returned to the level measured at

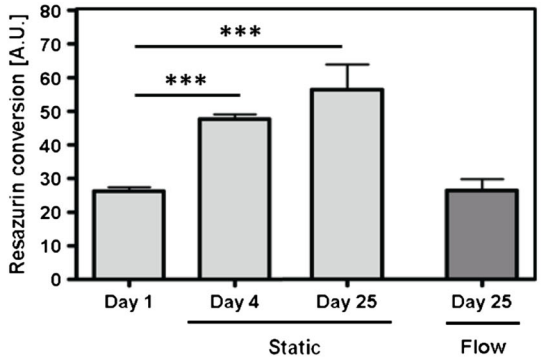

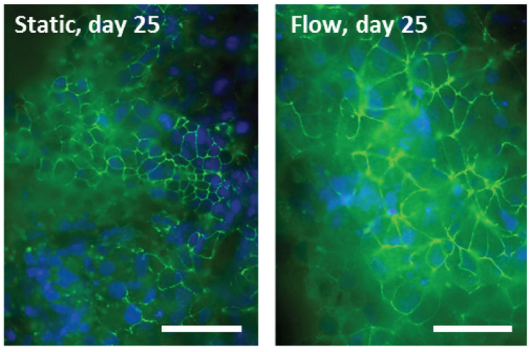

Figure 7. The effect of bioreactor flow culture on renal tubule test membranes. HK-2 cells were statically pre-cultured on bioactive UPy-PCL membranes for 4 days, followed by a culture period of 21 days, either under flow conditions inside a bioreactor or prolonged static culture in a well plate. Cell viability was monitored throughout the experiment via a non-invasive mitochondrial activity assay based on the conversion of resazurin (left). Error bars indicate standard error of mean. The significant increase (ANOVA, * indicates $p < 0.001$) in mitochondrial activity during the static pre-culture period (day 1 – day 4) remained present during the prolonged static culture (day 4 – day 25), whereas there was no difference measured between flow cultured membranes at day 25 and the initial culture at day 1 (two-tailed P value is 0.952, two-sample unpaired t-test). After the total culture period of 25 days, the cells were stained for ZO-1 (green, cell nuclei are in blue). The fluorescence micrographs show the presence of tight-junctions in both the static and flow culture. Scale bars represent 50 μM.**

DOI: 10.1002/term

day 1 after cell seeding. For comparative static cultures, the activity remained elevated after these 21 days (Figure 7). For static control cultures of HK-2 cells seeded in tissue culture-treated polystyrene 24-well plates, an increase in mitochondrial activity was observed over time. After activity reached a maximum, it remained at a constant level (see supporting information, Figure S4). At this plateau, unstructured, multilayered growth was observed. This indicated the tendency of these cells to lose their typical epithelial phenotype when cultured *in vitro*. In contrast, the cells cultured on bioactive UPy–PCL membranes, under both static and continuous flow conditions, were more homogeneously distributed compared to cultures on polystyrene. When comparing the culture conditions on the UPy–PCL membranes, live/dead staining showed similar cell viability for flow and static conditions, although the cells appeared bigger (in the *x*–*y* plane) on the flow-cultured membranes (see supporting information, Figure S5).

3.2.3.2. Cell morphology, gene expression and brush border enzyme activity. Immunofluorescent staining of zona occludens-1 (ZO-1) protein was performed to examine the effect of 21 days of flow culture inside the bioreactor, compared to continued static culture, on the morphology of a statically precultured epithelial cell layer. The typical ZO-1 staining, which is indicative of the desired tight, confluent and polarized epithelial morphology, was observed for both flow and static cultures (Figure 7). Similarly to what is seen with live/dead staining, the cells appeared larger (in the *x*–*y* plane) in the flow cultures than in the static cultures.

The effect of 21 days of flow culture on typical renal tubular epithelial gene expression was assessed by quantitative RT–PCR. HK-2 cells showed modulated expression levels of genes encoding for specialized membrane transporter proteins when compared to cultures after flow and static culture conditions (Figure 8a). Gene expression analysis implied a tendency towards enhanced

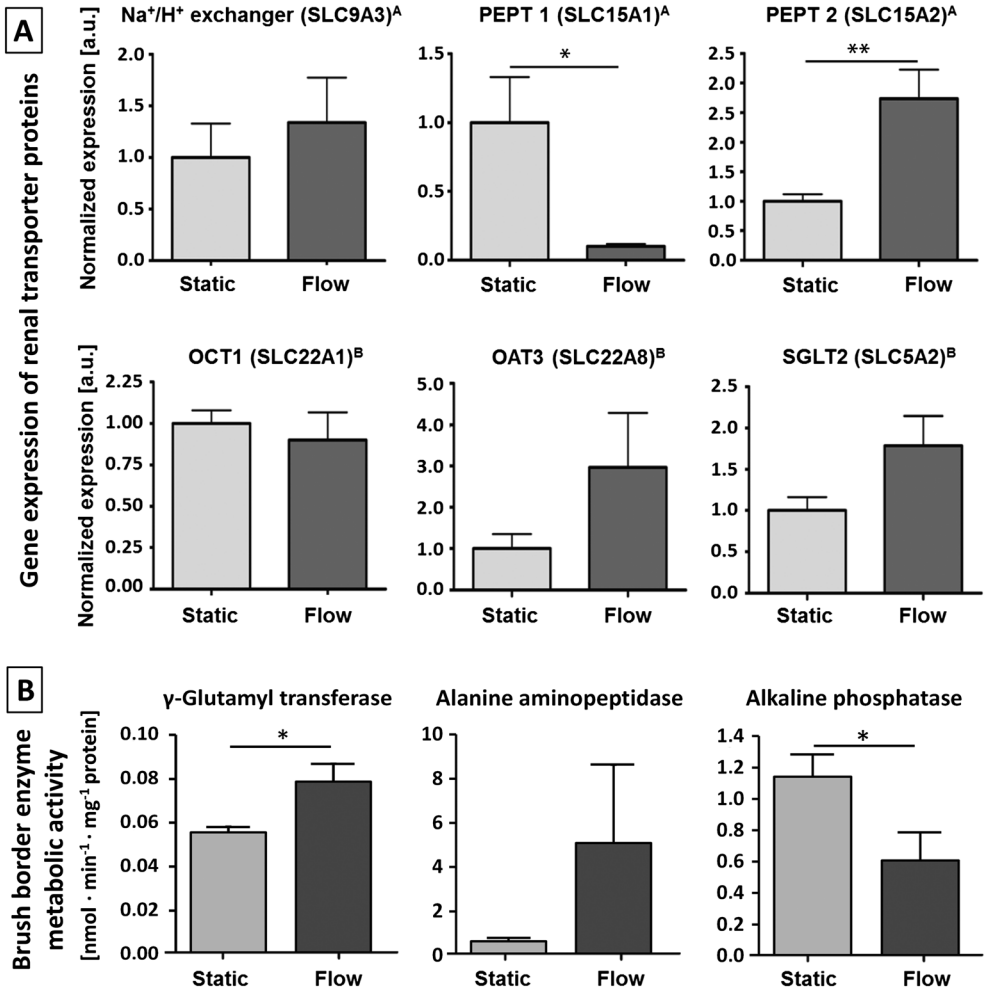

Figure 8. The effect of bioreactor flow culture on renal tubule test membranes. HK-2 cells were statically pre-cultured on bioactive UPy-PCL membranes for 4 days, followed by a culture period of 21 days, either under flow conditions inside a bioreactor or prolonged static culture in a well plate. Flow and static cultures are compared for: (A) RT-PCR expression levels of specific apical (A) and basolateral (B) membrane transporter proteins at the mRNA level (corresponding genes are indicated in brackets. Static $n=7$, flow $n=5$), and (B) activity of brush border enzymes, expressed as nmol substrate conversion per min, corrected for the amount of protein in the cell lysate (static $n=4$, flow $n=3$). Mean ± standard errors are reported. Significant differences are indicated by *($p<0.05$) and **($p<0.01$).

DOI: 10.1002/term

expression of the renal transporters *SGLT2*, Na^+/H^+ ATPase, *Pept 2* and *OAT 3*, but not *Pept1* and *OCT1*, after flow culture, indicating that the epithelial phenotype is better preserved when HK-2 cells are cultured under flow in our bioreactor set-up.

Also, the activity of brush border enzymes appeared modulated when compared to flow cultures with static cultures (Figure 8b). The 21 days of culture under flow conditions inside the bioreactor significantly increased the γ-glutamyl transferase activity of the HK-2 cells. The activity of alanine aminopeptidase strongly varied among the flow-cultured test membranes, whereas the static cultures all showed very similar, but generally lower, activity than flow cultures. This indicated an up-regulating effect of flow culture on this enzyme's activity. In contrast, for alkaline phosphatase the higher activity was observed for static cultures, but only when corrected for the amount of protein present in the cell lysate; a significantly higher protein content was observed for the flow cultures compared to the static cultures (see supporting information, Figure S6).

4. Discussion

Our goal was to create an *in vitro* mimic of the renal tubular epithelial cells' natural environment to allow the formation and study of functional bioartificial kidney tubule membranes for future medical applications. We combined a synthetic basement membrane mimic with an organotypical culture environment.

The majority of clinically relevant approaches that involve renal epithelial cells have focused on synthetic materials to substitute the BM, often combined with biological components. For example, in reported endeavours towards *in vitro* devices to complement haemodialysis treatments (Saito *et al.*, 2011; Humes *et al.*, 1999; Ni *et al.*, 2011), kidney tubule epithelial cells were seeded on the anti-adhesive synthetic materials that are employed in commercial haemofilters, coated with cell-adhesive, ECM-derived components. Studies on the application of renal epithelial cells in *in vitro* nephrotoxicity tests predominantly focused on the selection of cell-source and proper read-out parameters (Pfaller and Gstraunthaler, 1998; Li *et al.*, 2013) or on the development of a microfluidic device to generate an 'organ-on-a-chip' (Jang and Suh, 2010; Sciancalepore *et al.*, 2014; Baudoin *et al.*, 2007; Kelly *et al.*, 2013; Wei *et al.*, 2012), rather than on the development or selection of BM-substituting materials. Commercially available polymer surfaces, with or without biological coatings, were applied in these studies. The synthetic materials alone cannot provide the dynamic, bioactive nature or hierarchical structure of the BM. On the other hand, the use of natural components poses hurdles toward clinical translation of the envisioned applications, for example by their limited availability and variability of composition.

In our endeavours to mimic the basement membrane, we have focused on a completely synthetic approach, in which the supramolecular interactions between UPy-moieties play a prominent role. In earlier studies we showed that UPy-based supramolecular biomaterials are promising candidates for mimicking the BM, since UPy-functionalized polymers and UPy–peptides can be combined to form inherently dynamic biomaterials with tunable material properties and bioactive functions (Dankers *et al.*, 2010, 2011; Mollet *et al.*, 2014). Here we demonstrate that UPy-based biomaterials can also be applied to mimic the morphological characteristics of natural basement membranes. In UPy-functionalized polymer biomaterials, hierarchical self-assembly of UPy-moieties, i.e. UPy-dimerization, UPy-dimer stacking and stack aggregation, gives rise to well-defined nanoscale fibrous structures. Although a self-assembled nanofibrous structure has long been assumed to be present in electrospun microfibres of UPy-functionalized polymers, the AFM and WAXS data presented here (Figure 3) provide the first experimental data that support this assumption. Electrospinning of UPy-polymer biomaterials thus not only provides the opportunity to create porous, freestanding membranes, but also complements the self-assembled nanofibrillar structure with a microfibrous superstructure. Hence, UPy-polymers allow for the recreation of hierarchical fibrous morphologies, as found in natural basement membranes.

To screen and supplement our UPy-biomaterial electrospun membranes in their performance as *in vitro* basement membrane mimics for renal epithelial cells, we developed a bioreactor that provides an organotypical culture environment. The bioreactor provides separate flow of media to the apical and basal sides of a freely chosen flat support material, such as any membrane. The customized bioreactor was tested for a diversity of requirements in cell-employed assays. Monitoring of a culture inside the bioreactor by microscopy imaging was successfully demonstrated with objectives up to $\times 20$ magnification (Figure 5), which is appropriate for the monitoring of general features of the culture, such as cell density or confluence. This will in particular be a valuable tool for monitoring of the culture when using transparent culture supports inside the bioreactor that allow for brightfield microscopy. However, when applying opaque substrates such as our UPy–PCL membranes, fluorescent labelling of cells is needed to provide visual information by microscopy during culture inside the bioreactor. Non-invasive fluorescent staining, such as the staining of live cells with calcein, can provide visual access to the cells up to few cell passages. An alternative approach, which could provide stable fluorescence and enable monitoring of specific cell features, is genetically encoded labelling through transfection.

The bioreactor was designed with a separate chamber at each side of the membrane. Both chambers have their own flow inlet and outlet. This organotypical compartmentalization allows the separation of media flow on the apical and basal sides of the membrane. Besides the aim of stimulated polarization of renal epithelial cells, the compartmentalization allows the readout of cell functionality through diffusion and transport assays. This functionality was successfully demonstrated by the inulin

DOI: 10.1002/term

diffusion assay (Figure 6), which gives a measure of the integrity of the epithelial cell barrier. In a similar way, active transport studies can also be performed by applying, for example, a uraemic toxin at the basal volume and studying its transport towards the apical volume by the renal epithelial cells in the presence and absence of a transport inhibitor (Schophuizen *et al.*, 2013). When using fluorescently labelled compounds in the bioreactor, diffusion or transport could potentially also be monitored in real time, using fluorescence microscopy through the glass windows of both chambers. Furthermore, here the diffusion test was performed under static incubation conditions, whereas the bioreactor provides the opportunity to perform similar studies under flow conditions, which better resembles the renal epithelial niche. This offers advantages in comparison to the performance of such assays in commercial static culture set-ups with compartmentalized media, such as Transwell® (Corning) or Crowncell™ (Scafdex).

The bioreactor flow culture set-up allowed the culture of bioartificial kidney membranes under constant flow of media. Cultures of up to at least 21 days proved to be successful (Figure 7). This indicates suitable functionality of the bioreactor set-up according to several basic design criteria. It shows that the set-up can be assembled in a sterile way and free of leakage. Furthermore, no adverse effects were caused by air bubbles in the flow system, and the cells survived the handlings involved with membrane transfer into (when cells are seeded outside the bioreactor) and from the bioreactor. Cell viability was indicated by both mitochondrial activity assay and live/dead staining. The total mitochondrial activity for flow-cultured membranes was lower compared to that of static cultures. In previous experiments using primary proximal tubule epithelial cells on similar membranes, mitochondrial activity when cultured in another flow system was also found to be lower, as in static cultures (Dankers *et al.*, 2011). In correspondence with this study, observations of cell morphology by fluorescence microscopy revealed that cells cultured under flow conditions appear bigger (in the *x*–*y* plane). Hence, fewer cells are present on the same surface area. This might explain the lower total mitochondrial activity observed for these flow cultures, since total mitochondrial activity is an indirect measure for the amount of cells. HK-2 cells cultured under static conditions on tissue culture-treated polystyrene show abundant and unrestricted cell proliferation resulting in multilayered growth. This contributes to the loss of epithelial-specific phenotype for this cell line. Given the fact that the seeded cell density on the membranes was high enough to form an instant monolayer, the presented results might indicate that flow culture either helps to establish a stable cell turnover of continuously proliferating HK-2 cells, or that HK-2 cells cultured under flow conditions regained characteristic contact inhibition, preventing them from abundant and unrestricted proliferation, as compared to static cultures. The loss of contact inhibition and subsequent overgrowing from a monolayer to multilayer morphology was mentioned by Saito *et al.* (2011) as the main cause of suboptimal functioning of a bioartificial renal tubule device consisting of a hollow-fibre module and human proximal tubule epithelial cells (Saito *et al.*, 2011). These results, shown with our supramolecular newly developed bioreactor, are thus promising towards improved *in vitro* applications of renal epithelial cells.

HK-2 cells on bioactive UPy–PCL membranes furthermore showed both modulated brush border enzyme activity and expression levels of membrane transporter proteins, when compared to culture for 21 days under flow conditions to static culture conditions (Figure 8). The enzymatic activities were corrected for the amount of total protein present in the cell lysate of the cultures. Remarkably, the protein content in flow cultures was significantly higher than in static cultures. As a result, the overall, non-protein corrected activity of all three tested brush border enzymes was either equal to, or higher than, the activity in static cultures (see supporting information, Figure S6). From the presented results we cannot distinguish between down-regulated enzymatic activity and transporter protein expression under static conditions, or up-regulation under flow conditions. Nevertheless, the results do indicate preserved or even regained renal epithelial phenotype under flow culture conditions in our bioreactor.

For the described cell-based tests, HK-2 cells were used as a model for renal tubular epithelial cells. Although these cells might not be the most appropriate cells for future clinical applications, they proved sufficient for current tests, in which primarily the function of the bioreactor was assessed. In future experiments, employing the bioreactor as culture and read-out tool for renal epithelial cell functionality on new UPy-biomaterial membrane designs, other cell sources might prove more useful, such as primary cells or immortalized cell lines, with improved preservation of *in vivo*-like characteristics (Wilmer *et al.*, 2010; Jansen *et al.*, 2014).

5. Conclusions

With the aim of creating a bioartificial *in vitro* mimic of the renal tubular epithelial cells' natural environment, we combined synthetic substitutes for the basement membrane and an organotypical culture environment. For mimicry of the basement membrane, we have focused on a promising class of synthetic materials; supramolecular biomaterials based on UPy-moieties. Here we demonstrated the hierarchical fibrous architecture, from nanoscale to microscale, of electrospun membranes of a UPy-polymer based biomaterial. This provides morphological mimicry of natural basement membranes. As an organotypical culture environment, we have developed a bioreactor system in which the bioartificial kidney membrane can be exposed to a continuous flow of separate media on both apical and basal sides, and which furthermore allows *in situ* monitoring of the membrane culture via microscopy. HK-2 cells were successfully cultured for

DOI: 10.1002/term

21 days under flow conditions inside the bioreactor. The results indicate a positive effect of the culture under flow conditions inside the bioreactor. Characteristics of the differentiated and functional renal epithelial phenotype are preserved or regained when compared to static cultures. We intend to employ the bioreactor in combination with new variants of BM mimics and relevant cells. This will aid the formation, study and screening of living bioartificial kidney membranes for future *in vitro* clinical applications, such as improved haemodialysis treatments and nephrotoxicity tests.

Conflict of interest

The authors have declared that there is no conflict of interest.

Acknowledgements

The authors gratefully thank Peter Neerincx and Han Meijer for their help with the initial designs for the bioreactor prototype, Patrick de Laat for his ideas and work concerning the technical aspects and the actual realization of the bioreactor, and Bart van Overbeeke for photography of the bioreactor. We thank Eva Wisse for the synthesis of the UPy–peptides, Wilco Appel for AFM imaging, Giuseppe Portale for help with WAXS measurements and data analysis, and Bert Meijer for useful discussions. The research leading to these results has received funding from the European Research Council (Grant No. FP7/2007–2013; ERC Grant Agreements Nos 308045 and 246829). This research forms part of the Project P3.01 BioKid of the research programme of the BioMedical Materials Institute, co-founded by the Dutch Ministry of Economic Affairs. A financial contribution from the Dutch Kidney Foundation is gratefully acknowledged.

References

Aebischer P, Ip TK, Panol G *et al.* 1987; The bioartificial kidney: progress towards an ultrafiltration device with renal epithelial cells processing. *Life Support Syst* **5**: 159–168.

Aida T, Meijer EW, Stupp SI. 2012; Functional supramolecular polymers. *Science* **335**: 813–817.

Andersson AS, Bäckhed F, von Euler A *et al.* 2003; Nanoscale features influence epithelial cell morphology and cytokine production. *Biomaterials* **24**: 3427–3436.

Aota SI, Nomizu M, Yamada KM. 1994; The short amino acid sequence Pro–His–Ser–Arg–Asn in human fibronectin enhances cell-adhesive function. *J Biol Chem* **269**: 24756–24761.

Appel WPJ. 2011; Synthesis, Characterization and Applications of Quadrupole Hydrogen Bonded Polymers. Thesis, Eindhoven University of Technology.

Appel WPJ, Portale G, Wisse E *et al.* 2011; Aggregation of ureido-pyrimidinone supramolecular thermoplastic elastomers into nanofibers: a kinetic analysis. *Macromolecules* **44**: 6776–6784.

Baudoin R, Griscom L, Monge M *et al.* 2007; Development of a renal microchip for *in vitro* distal tubule models. *Biotechnol Prog* **23**: 1245–1253.

Bettinger CJ, Langer R, Borenstein JT. 2009; Engineering substrate micro- and nanotopography to control cell function. *Angew Chem Int Ed Engl* **48**: 5406–5415.

Bradford MM. 1976; A rapid and sensitive method for the quantitation of microgram quantities of protein utilizing the principle of protein–dye binding. *Anal Biochem* **72**: 248–254.

Dankers PYW, Boomker JM, Huizinga-der Vlag A *et al.* 2010; The use of fibrous, supramolecular membranes and human tubular cells for renal epithelial tissue engineering: towards a suitable membrane for a bioartificial kidney. *Macromol Biosci* **10**: 1345–1354.

Dankers PYW, Boomker JM, Huizinga-van der Vlag A *et al.* 2011; Bioengineering of living renal membranes consisting of hierarchical, bioactive supramolecular meshes and human tubular cells. *Biomaterials* **32**: 723–733.

Ferrell N, Desai RR, Fleischman AJ *et al.* 2010; A microfluidic bioreactor with integrated transepithelial electrical resistance (TEER) measurement electrodes for evaluation of renal epithelial cells. *Biotechnol Bioeng* **107**: 707–716.

Fissell WH, Manley S, Westover A *et al.* 2006; Differentiated growth of human renal tubule cells on thin-films nanostructured materials. *ASAIO J* **52**: 221–227.

Fujita Y, Kakuta T, Asano M *et al.* 2002; Evaluation of Na^+ active transport and morphological changes for bioartificial renal tubule cell device using Madin–Darby canine kidney cells. *Tissue Eng* **8**: 13–24.

Humes HD. 2000; Bioartificial kidney for full renal replacement therapy. *Semin Nephrol* **20**: 71–82.

Humes HD, Mackay SM, Funke AJ *et al.* 1999; Tissue engineering of a bioartificial renal tubule assist device: *in vitro* transport and metabolic characteristics. *Kidney Int* **55**: 2502–2514.

Iwamoto Y, Robey FA, Graf J *et al.* 1987; YIGSR, a synthetic laminin pentapeptide, inhibits experimental metastasis formation. *Science* **238**: 1132–1134.

Jansen J, Schophuizen CM, Wilmer MJ *et al.* 2014; A morphological and functional comparison of proximal tubule cell lines established from human urine and kidney tissue. *Exp Cell Res* **323**: 87–99.

Jang KJ, Suh KY. 2010; A multi-layer microfluidic device for efficient culture and analysis of renal tubular cells. *Lab Chip* **10**: 36–42.

Kautz H, van Beek DJM, Sijbesma RP *et al.* 2006; Cooperative end-to-end and lateral hydrogen-bonding motifs in supramolecular thermoplastic elastomers. *Macromolecules* **39**: 4265–4267.

Kelly EJ, Wang Z, Voellinger JL *et al.* 2013; Innovations in preclinical biology: *ex vivo* engineering of a human kidney tissue microperfusion system. *Stem Cell Res Ther* **4**(suppl 1): S17.

Kieltyka RE, Bastings MMC, van Almen GC *et al.* 2012; Modular synthesis of supramolecular ureidopyrimidinone–peptide conjugates using an oxime ligation strategy. *Chem Commun* **48**: 1452–1454.

Kim SS, Penkala R, Abrahimi P. 2007; A perfusion bioreactor for intestinal tissue engineering. *J Surg Res* **142**: 327–331.

Kirkpatrick J. 2014; Developing cellular systems *in vitro* to simulate regeneration. *Tissue Eng A* **20**: 1355–1357.

Li Y, Oo ZY, Chang SY *et al.* 2013; An *in vitro* method for the prediction of renal proximal tubular toxicity in humans. *Toxicol Res* **2**: 352–365.

Madara JL, Dharmsathaphorn K. 1985; Occluding junction structure–function relationships in a cultured epithelial monolayer. *J Cell Biol* **101**: 2124–2133.

Miller C, George S, Niklason L. 2010; Developing a tissue-engineered model of the human bronchiole. *J Tissue Eng Regen Med* **4**: 619–627.

Minuth WW, Denk L. 2015; Bridging the gap between traditional cell cultures and bioreactors applied in regenerative medicine: practical experiences with the MINUSHEET perfusion culture system. *Cytotechnology*. DOI:10.1007/s10616–015–9873-x. (in press)

Minuth WW, Denk L, Roessger A. 2009; Gradient perfusion culture-simulating a tissue-specific environment for epithelia in biomedicine. *J Epithel Biol Pharmacol* **2**: 1–13.

Mollet BB, Comellas-Aragonès M, Spiering AJH *et al.* 2014; A modular approach to easily processable supramolecular bilayered scaffolds with tailorable properties. *J Mater Chem B* **2**: 2483–2493.

Ni M, Teo J, Ibrahim MS *et al.* 2011; Characterization of membrane materials and membrane coatings for bioreactor units of bioartificial kidneys. *Biomaterials* **32**: 1465–1476.

Ozgen N, Terashima M, Aung T *et al.* 2004; Evaluation of long-term transport ability of a bioartificial renal tubule device using LLC-PK1 cells. *Nephrol Dial Transpl* **19**: 2198–2207.

Pfaller W, Gstraunthaler G. 1998; Nephrotoxicity testing *in vitro* – what we know and what we need to know. *Environ Health Perspect* **106**: 559–569.

Pierschbacher MD, Ruoslahti E. 1984; Cell attachment activity of fibronectin can be duplicated by small synthetic fragments of the molecule. *Nature* **309**: 30–33.

Ryan MJ, Johnson G, Kirk J *et al.* 1994; HK-2: An immortalized proximal tubule

epithelial cell line from normal adult human kidney. *Kidney Int* **45**: 48–57.
Saito A, Sawada K, Fujimura S. 2011; Present status and future perspectives on the development of bioartificial kidneys for the treatment of acute and chronic renal failure patients. *Hemodial Int* **15**: 183–192.
Schophuizen CMS, De Napoli IE, Jansen J *et al*. 2015; Development of a living membrane comprising a functional human renal proximal tubule cell monolayer on polyethersulfone polymeric membrane. *Acta Biomater* **14**: 22–32. DOI:10.1016/j.actbio.2014.12.002.
Schophuizen CMS, Wilmer MJ, Jansen J *et al.* 2013; Cationic uremic toxins affect human renal proximal tubule cell functioning through interaction with the organic cation transporter. *Pflüg Arch Eur J Physiol* **465**: 1701–1714.
Sciancalepore AG, Sallustio F, Girardo S *et al.* 2014; A bioartificial renal tubule device embedding human renal stem/progenitor cells. *PLoS One* **9**: e87496.
Sijbesma RP, Beijer FH, Brunsveld L *et al*. 1997; Reversible Polymers Formed from Self-Complementary Monomers Using Quadruple Hydrogen Bonding. *Science* **278**: 1601–1604.
Smith HW. 1951; The Kidney: Structure and Function in Health and Disease, Oxford University Press: Oxford.
Söntjens SHM, Sijbesma RP, van Genderen MHP *et al.* 2000; Stability and lifetime of quadruply hydrogen-bonded 2-ureido-4[1*H*]-pyrimidinone dimers. *J Am Chem Soc* **122**: 7487–7493.
Staatz WD, Fok KF, Zutter MM *et al.* 1991; Identification of a tetrapeptide recognition sequence for the $\alpha 2\beta 1$ integrin in collagen. *J Biol Chem* **266**: 7363–7367.
Sun T, Donoghue PS, Higginson JR *et al.* 2012; A miniaturized bioreactor system for the evaluation of cell interaction with designed substrates in perfusion culture. *J Tissue Eng Regen Med* **6**(suppl 3): s4–s14.
Timpl R. 1996; Macromolecular organization of basement membranes. *Curr Opin Cell Biol* **8**: 618–624.
Timpl R, Brown JC. 1996; Supramolecular assembly of basement membranes. *Bioessays* **18**: 123–132.
Tiong HY, Huang P, Xiong S *et al.* 2014; Drug-induced nephrotoxicity: clinical impact and preclinical *in vitro* models. *Mol Pharm* **11**: 1933–1948.
Van Beek DJM, Spiering AJH, Peters GWM *et al.* 2007; Unidirectional dimerization and stacking of ureidopyrimidinone end groups in polycaprolactone supramolecular polymers. *Macromolecules* **40**: 8464–8475.
Wietor JL, van Beek DJM, Peters GW *et al.* 2011; Effects of branching and crystallization on rheology of polycaprolactone supramolecular polymers with ureidopyrimidinone end groups. *Macromolecules* **44**: 1211–1219.
Wilmer MJ, Saleem MA, Masereeuw R *et al.* 2010; Novel conditionally immortalized human proximal tubule cell line expressing functional influx and efflux transporters. *Cell Tissue Res* **339**: 449–457.
Wei Z, Amponsah PK, Al-Shatti M *et al.* 2012; Engineering of polarized tubular structures in a microfluidic device to study calcium phosphate stone formation. *Lab Chip* **12**: 4037–4040.

Supporting information

Additional supporting information may be found in the online version of this article at the publisher's web site.

Figure S1. Transmembranal FITC–inulin diffusion assay performed using the bioreactor
Figure S2. Fluorescence micrographs of HK-2 cells on a UPy–PCL membrane inside the bioreactor after live/dead staining over time
Figure S3. Fluorescence micrographs of HK-2 cells show the formation of tight junctions over time
Figure S4. Resazurin assays were performed over time to monitor the total mitochondrial activity of HK-2 cell cultures on tissue culture-treated polystyrene in a standard 24-well plate
Figure S5. Fluorescence micrographs of live/dead-stained HK-2 cells cultured on bioactive UPy–PCL membranes for varying times and conditions
Figure S6. HK-2 cells were cultured on bioactive UPy–PCL membranes for varying times and conditions
Table S1. Real-time PCR primers for human membrane proteins